

On the capacity of TDMA downlink with a reconfigurable intelligent surface

Donatella Darsena, *Senior Member, IEEE* and Francesco Verde, *Senior Member, IEEE*

Abstract—We provide accurate approximations of the sum-rate capacity of a time-division multiple access (TDMA) downlink, when a reconfigurable intelligent surface (RIS) assists the transmission from a single-antenna base station (BS) to K single-antenna user equipments (UEs). We consider the fading effects of both the direct (i.e., BS-to-UEs) and reflection (i.e., BS-to-RIS-to-UEs) links, by developing two approximations: the former one is based on hardening of the reflection channel for large values of the number Q of meta-atoms at the RIS; the latter one relies on the distribution of the sum of Nakagami variates and does not require channel hardening. Our derivations show the dependence of the sum-rate capacity as a function of both K and Q , as well as to establish a comparison with a TDMA downlink without an RIS. Numerical results corroborate the accuracy of the proposed approximations and the validity of the mathematical analysis.

Index Terms—Downlink transmission, reconfigurable intelligent surface (RIS), time-division multiple access (TDMA).

I. INTRODUCTION

IN this letter, we consider a downlink channel in which a *reconfigurable intelligent surface (RIS)* is employed to assist the transmission from a single-antenna transmitter towards $K \gg 1$ single-antenna user equipments (UEs). An RIS is a metasurface composed of sub-wavelength meta-atoms, whose reflection coefficients can be designed via software in order to suitably manipulate the impinging signal [1]. For instance, beam steering and high directivity can be obtained by changing the state of meta-atoms at different spatial positions on the metasurface. Relying on the feasibility of engineering the meta-atoms, the wireless propagation environment might be programmed by optimizing on-the-fly the reflecting properties of an RIS to achieve different network-wide aims [2], [3].

Time-division multiple-access (TDMA) is a simple and effective transmission technique - widely used in commercial communication systems - which allows a base station (BS) to transmit to only one user at a time. TDMA has been shown to achieve the sum-rate capacity (maximum throughput) of the single-antenna downlink channel [4]. Considering the widespread use of TDMA, a relevant question to ask is the

following: *How large of a performance boost does RIS-aided TDMA downlink provide over its conventional (i.e., without RIS) counterpart in terms of sum-rate?* The scaling law of the sum-rate capacity of a Gaussian downlink with many users K using TDMA has been deeply studied without an RIS [5]. A similar study for an RIS-aided downlink with a large number of users K and meta-atoms Q has not been carried out yet.

We focus on the sum-rate capacity, achievable using TDMA, by considering a system where all the relevant channel state information is available at the BS and UEs. We develop an approximation of the sum-rate capacity by invoking hardening of the reflection channel in the large Q limit, which allows to readily unveil the scaling laws as a function of K and Q . Furthermore, we provide a very accurate approximation of the sum-rate capacity without invoking channel hardening, which is based on the sum of Nakagami variates. We also investigate the interplay between the gain offered by the RIS and the selection diversity among users.

II. SIGNAL MODEL AND PRELIMINARIES

The downlink transmission among the BS and K UEs is assisted by a digitally programmable RIS working in reflection mode, which is made of Q spatial meta-atoms that can be independently and dynamically controlled by digital logic devices [1].¹ The channel between the BS and the RIS is assumed to be characterized by a dominant line-of-sight component, which is modeled as $\mathbf{g} = \sigma_g \mathbf{a}_{\text{RIS}}$, with pathloss σ_g^2 and spatial signature $\mathbf{a}_{\text{RIS}} \triangleq [1, e^{j \frac{2\pi}{\lambda_0} d_{\text{RIS}} \cos(\vartheta_{\text{RIS}})}, \dots, e^{j \frac{2\pi}{\lambda_0} (Q-1) d_{\text{RIS}} \cos(\vartheta_{\text{RIS}})}]_{\text{T}}$, where $\lambda_0 = c/f_0$ is the wavelength, c is the speed of the light in the medium, d_{RIS} is the inter-element spacing at the RIS, and ϑ_{RIS} is the angle-of-arrival (AoA).

All the other relevant links are modeled as narrowband frequency-flat channels. Specifically, for $k \in \{1, 2, \dots, K\}$, $h_k \sim \mathcal{CN}(0, \sigma_{h_k}^2)$ models the low-pass equivalent channel response from the BS to UE k , whereas $\mathbf{f}_k \sim \mathcal{CN}(\mathbf{0}_Q, \sigma_{f_k}^2 \mathbf{I}_Q)$, represents the low-pass equivalent channel response from the RIS to the k -th UE. The parameters $\sigma_{h_k}^2$ and $\sigma_{f_k}^2$ are the large-scale geometric path losses of the links seen by the k -th UE with respect to the BS and the RIS, respectively.

We customarily assume that each UE uses standard timing synchronization with respect to its direct link. After matched filtering and sampling at the baud rate, the discrete-time

Manuscript received May 19, 2023; accepted xx yy 2023. Date of publication xx yy 2023; date of current version xx yy 2023. This work was partially supported by the European Union under the Italian National Recovery and Resilience Plan (NRRP) of NextGenerationEU, partnership on “Telecommunications of the Future” (PE00000001 - program “RESTART”). The associate editor coordinating the review of this article and approving it for publication was Prof. XX. YY. (*Corresponding author: Francesco Verde.*)

F. Verde and D. Darsena are with the Department of Electrical Engineering and Information Technology, University Federico II, Naples I-80125, Italy [e-mail: (f.verde, darsena)@unina.it]. The Authors are also with National Inter-University Consortium for Telecommunications (CNIT).

Digital Object Identifier xxxxxxxxxxxxxxxxxxxx.

¹We consider a space-only RIS. Space-time RIS is studied in [6].

baseband signal received at the k -th user reads as

$$r_k = c_k^* \left(\sum_{u=1}^K \sqrt{\mathcal{P}_u} s_u \right) + v_k \quad (1)$$

where the *overall* channel gain seen by the k -th UE is

$$c_k \triangleq h_k + \mathbf{g}^H \mathbf{\Gamma}^* \mathbf{f}_k \in \mathbb{C}, \quad \text{for } k \in \{1, 2, \dots, K\} \quad (2)$$

with the q -th diagonal entry of $\mathbf{\Gamma} \triangleq \text{diag}(\gamma_1, \gamma_2, \dots, \gamma_Q)$ representing the reflection coefficient of the q -th meta-atom, s_u being the information-bearing symbol intended for the u -th user with corresponding transmit power \mathcal{P}_u , and $v_k \sim \mathcal{CN}(0, 1)$ is the noise sample at the output of the matched filter, with v_{k_1} statistically independent of v_{k_2} , for $k_1 \neq k_2$. The transmitted symbols s_1, s_2, \dots, s_K are independent and identically distributed (i.i.d.) complex circular zero-mean unit-variance random variables. The couple (h_k, \mathbf{f}_k) is independent of both v_k and s_k , $\forall k \in \{1, 2, \dots, K\}$.

The *sum-rate capacity* (in bits/s/Hz) is defined as follows

$$\mathcal{C}_{\text{sum}} = \max_{\substack{\mathcal{P}_1, \mathcal{P}_2, \dots, \mathcal{P}_K \\ \gamma_1, \gamma_2, \dots, \gamma_Q}} \sum_{k=1}^K \log_2(1 + \text{SINR}_k) \quad (3)$$

with $\text{SINR}_k \triangleq \mathcal{P}_k |c_k|^2 / \left(|c_k|^2 \sum_{u \neq k} \mathcal{P}_u + 1 \right)$ denoting the signal-to-interference-plus-noise ratio at UE k , subject to the *transmit power constraint* $\sum_{k=1}^K \mathcal{P}_k \leq \mathcal{P}_{\text{TX}}$, with $\mathcal{P}_{\text{TX}} > 0$ being the (fixed) maximum allowed transmit power, and the *global passivity constraint* $\|\gamma\|^2 \leq Q$ at the RIS [7]. For a lossless RIS, the latter constraint yields $\|\gamma\|^2 = Q$.

Given the reflection vector $\gamma \triangleq [\gamma_1, \gamma_2, \dots, \gamma_Q]^H \in \mathbb{C}^Q$ of the RIS, the sum-rate capacity is equal to the largest single-user capacity in the system [4], that is, the resource allocation policy is the TDMA strategy: $\mathcal{P}_k = \mathcal{P}_{\text{TX}}$ if $k = k_{\text{max}}$, $\mathcal{P}_k = 0$ otherwise, with $k_{\text{max}} \triangleq \arg \max_{k \in \{1, 2, \dots, K\}} |c_k|^2$. According to (2), the corresponding sum-rate capacity is

$$\mathcal{C}_{\text{sum}} = \log_2(1 + \mathcal{P}_{\text{TX}} \alpha_{\text{opt}}) \quad (4)$$

with

$$\alpha_{\text{opt}} \triangleq \max_{\substack{k \in \{1, 2, \dots, K\} \\ \gamma \in \mathbb{C}^Q: \|\gamma\|^2 = Q}} |h_k|^2 + 2 \Re \{ \beta_k^H \gamma \} + \gamma^H \mathbf{B}_k \gamma \quad (5)$$

where $\beta_k \triangleq h_k \text{diag}(\mathbf{f}_k^*) \mathbf{g} \in \mathbb{C}^Q$ and we have defined the Hermitian matrix $\mathbf{B}_k \triangleq \text{diag}(\mathbf{f}_k^*) \mathbf{g} \mathbf{g}^H \text{diag}(\mathbf{f}_k) \in \mathbb{C}^{Q \times Q}$. Solution of (5) is provided by the following lemma.

Lemma 2.1: Under the assumption that $\|\gamma\|^2 = Q$, the cost function in (5) can be upper bounded as follows

$$|h_k|^2 + 2 \Re \{ \beta_k^H \gamma \} + \gamma^H \mathbf{B}_k \gamma \leq \left(|h_k| + \sqrt{Q} \|\text{diag}(\mathbf{f}_k^*) \mathbf{g}\| \right)^2$$

where the equality holds if and only if

$$\gamma \equiv \gamma_{\text{opt}} \triangleq \sqrt{Q} \frac{h_k \text{diag}(\mathbf{f}_k^*) \mathbf{g}}{|h_k| \|\text{diag}(\mathbf{f}_k^*) \mathbf{g}\|}. \quad (6)$$

Proof: The proof comes from $\Re\{x\} \leq |x| \forall x \in \mathbb{C}$, the Cauchy-Schwarz inequality, and the Rayleigh-Ritz theorem. ■

As a consequence of Lemma 2.1, eq. (5) ends up to

$$\alpha_{\text{opt}} = \max_{k \in \{1, 2, \dots, K\}} \left(|h_k| + \sqrt{Q} \|\text{diag}(\mathbf{f}_k^*) \mathbf{g}\| \right)^2. \quad (7)$$

III. THEORETICAL PERFORMANCE ANALYSIS

By applying channel coding across channel coherence intervals (i.e., over an ‘‘ergodic’’ interval of channel variation with time), the *average* sum-rate capacity is given by

$$\bar{\mathcal{C}}_{\text{sum}} \triangleq \mathbb{E}[\mathcal{C}_{\text{sum}}] = \int_0^{+\infty} \log_2(1 + \mathcal{P}_{\text{TX}} \alpha) f_{\alpha_{\text{opt}}}(\alpha) d\alpha \quad (8)$$

where $f_{\alpha_{\text{opt}}}(\alpha)$ is the probability density function (pdf) of the non-negative random variable α_{opt} in (7).

For simplicity, we consider the case in which the users approximately experience the same large-scale geometric path loss, i.e., the parameters $\sigma_{h_k}^2$ and $\sigma_{f_k}^2$ do not depend on k , i.e., $\sigma_{h_k}^2 \equiv \sigma_h^2$ and $\sigma_{f_k}^2 \equiv \sigma_f^2$, $\forall k \in \{1, 2, \dots, K\}$, which will be referred to as the case of *homogeneous* users.² In the case of homogeneous users, the random variable α_{opt} is the maximum of K i.i.d. random variables and its pdf can be computed as follows

$$f_{\alpha_{\text{opt}}}(\alpha) = K f_{X_k}(\alpha) [F_{X_k}(\alpha)]^{K-1} \quad (9)$$

where $f_{X_k}(x)$ and $F_{X_k}(x)$ denote the pdf and the cumulative distribution function (cdf) of the random variable $X_k \triangleq Z_k^2$, with $Z_k \triangleq Z_k^{(1)} + Z_k^{(2)}$, $Z_k^{(1)} \triangleq |h_k|$, and $Z_k^{(2)} \triangleq \sigma_g \sqrt{Q} \|\mathbf{f}_k\|$.

The distribution of the random variable $Z_k^{(1)}$ does not depend on the number Q of meta-atoms: it is a Rayleigh-distributed random variable or, equivalently, it can be seen as a Nakagami random variable with shape parameter $m = 1$ and scale parameter $\Omega = \sigma_h^2$ [8]. On the other hand, the distribution of $Z_k^{(2)}$ strongly depends on Q . Indeed, it can be readily verified that $Z_k^{(2)}$ is a Nakagami random variable with shape parameter $m = Q$ and scale parameter $\Omega = \sigma_f^2 \sigma_g^2 Q^2$, whose mean and variance are given by (see, e.g., [8])

$$\mathbb{E}[Z_k^{(2)}] = \sigma_f \sigma_g \sqrt{Q} \frac{\Gamma(Q + \frac{1}{2})}{\Gamma(Q)} \approx \sigma_f \sigma_g Q \quad (10)$$

$$\text{VAR}[Z_k^{(2)}] = \sigma_f^2 \sigma_g^2 Q^2 \left\{ 1 - \frac{1}{Q} \left[\frac{\Gamma(Q + \frac{1}{2})}{\Gamma(Q)} \right]^2 \right\} \approx \frac{\sigma_f^2 \sigma_g^2 Q}{4} \quad (11)$$

where $\Gamma(x) \triangleq \int_0^{+\infty} t^{x-1} e^{-t} dt$, with $x > 0$, is the gamma function, which ends up to $\Gamma(x) = (x-1)!$ when x is a (positive) integer, whereas the approximations come from the Stirling’s series of the quotient $\Gamma(Q + \frac{1}{2})/\Gamma(Q)$ [9] and they hold for very large Q . Trying to work with (9) for evaluating (8) is numerically difficult even for small values of K . For such a reason, we apply extreme value theory [10] to calculate the distribution of α_{opt} when K is sufficiently large (i.e., greater than 10). As $K \rightarrow \infty$, the random variable α_{opt} convergences in distribution [11] to the Gumbel distribution:

$$\lim_{K \rightarrow \infty} F_{\alpha_{\text{opt}}}(\alpha) = \exp \left[-e^{-\frac{\alpha - b_K}{a_K}} \right] \quad (12)$$

where $F_{\alpha_{\text{opt}}}(\alpha)$ is the cdf of α_{opt} and

$$b_K \triangleq F_{X_k}^{-1} \left(1 - \frac{1}{K} \right), \quad a_K \triangleq \frac{1 - F_{X_k}(b_K)}{f_{X_k}(b_K)} = \frac{1}{K f_{X_k}(b_K)} \quad (13)$$

²From a physical viewpoint, this happens when the users form a *cluster*, wherein the distances between the different UEs are negligible with respect to the distance between the transmitter and the RIS.

provided that the cdf of X_k is a von Mises function [12], i.e.,

$$\lim_{\alpha \rightarrow +\infty} \left[\frac{1 - F_{X_k}(\alpha)}{f_{X_k}^2(\alpha)} \right] \frac{d}{d\alpha} f_{X_k}(\alpha) = -1. \quad (14)$$

The proof of this result relies on the limit laws for maxima [10]. On the basis of (12), eq. (8) can be explicated as

$$\bar{c}_{\text{sum}} \asymp \frac{1}{a_K} \int_0^{+\infty} \log_2(1 + \mathcal{P}_{\text{TX}} \alpha) \cdot e^{-\frac{\alpha - b_K}{a_K}} \exp \left[-e^{-\frac{\alpha - b_K}{a_K}} \right] d\alpha \quad (15)$$

with $x \asymp y$ indicating that $\lim_{K \rightarrow +\infty} x/y = 1$. By using the Maclaurin series of the exponential function, the integral (15) can be rewritten [12, Appendix C] as follows

$$\bar{c}_{\text{sum}} \asymp \frac{1}{\ln 2} \sum_{i=0}^{+\infty} \frac{(-1)^i}{(i+1)!} e^{\frac{(i+1)(1+b_K \mathcal{P}_{\text{TX}})}{a_K \mathcal{P}_{\text{TX}}}} P \left(\frac{i+1}{a_K \mathcal{P}_{\text{TX}}}, 0 \right) \quad (16)$$

where $P(x, a) \triangleq \frac{1}{\Gamma(a)} \int_0^x t^{a-1} e^{-t} dt$ is the (regularized) lower incomplete gamma function, with $a \geq 0$. The infinite sum in (16) can be suitably truncated for finite number of terms.

As a by-product, the asymptotic distribution (12) allows one to statistically characterize the *receive* signal-to-noise ratio (SNR) of the user selected for scheduling, which is defined as $\rho_{\text{sum}} \triangleq \mathcal{P}_{\text{TX}} \alpha_{\text{opt}}$. Indeed, the statistical properties of ρ_{sum} can be studied by looking at the moments and order statistics of the Gumbel distribution. In particular, we can readily derive the average receive SNR $\bar{\rho}_{\text{sum}} \triangleq \mathbb{E}[\rho_{\text{sum}}] = \mathcal{P}_{\text{TX}} \mathbb{E}[\alpha_{\text{opt}}]$ from the mean of the Gumbel distribution, thus yielding

$$\bar{\rho}_{\text{sum}} = \mathcal{P}_{\text{TX}} (b_K + C a_K) \quad (17)$$

with $C \approx 0.5772$ being the Euler-Mascheroni constant.

The pdf or cdf of X_k must be derived to evaluate \bar{c}_{sum} by using either (8)-(9) or (16). In a downlink *without* an RIS, the random variable $X_k = [Z_k^{(1)}]^2 = |h_k|^2$ is exponentially distributed with mean σ_h^2 . In this case, it follows from (13) that $b_K = \sigma_h^2 \ln(K)$ and $a_K = \sigma_h^2$. From (17), the average receive SNR in an RIS-unaided TDMA downlink is

$$\bar{\rho}_{\text{sum}}^{\text{w/o RIS}} = \mathcal{P}_{\text{TX}} \sigma_h^2 [C + \ln(K)] \Rightarrow \lim_{K \rightarrow +\infty} \frac{\bar{\rho}_{\text{sum}}^{\text{w/o RIS}}}{\ln(K)} = \mathcal{P}_{\text{TX}} \sigma_h^2$$

which benefits by a factor of $\ln(K)$ asymptotically for large K (so-called *multiuser diversity effect*), and $\bar{c}_{\text{sum}}^{\text{w/o RIS}}$ increases double logarithmically in K [5]. On the other hand, in an RIS-aided downlink, the random variable X_k is the square of the sum of $Z_k^{(1)} = |h_k|$ and $Z_k^{(2)} = \sigma_g \sqrt{Q} \|\mathbf{f}_k\|$. In this case, to approximate the distribution of X_k , we distinguish two cases: in the former one, we assume that the reflection channel from the RIS to each UE hardens for sufficiently large values of Q ; in the latter one, we derive a more general approximation that does not require hardening of the reflection channel.

A. Approximation 1: Hardening of the reflection channel

The k -th reflection channel hardens [13] if $Z_k^{(2)}/\mathbb{E}[Z_k^{(2)}]$ converges in probability to 1, as $Q \rightarrow +\infty$, for each $k \in \{1, 2, \dots, K\}$. Based on the Markov inequality

[14], a sufficient condition for the hardening of $Z_k^{(2)}$ is $\text{VAR}[Z_k^{(2)}]/\mathbb{E}^2[Z_k^{(2)}] \rightarrow 0$, as $Q \rightarrow +\infty$. By virtue of (10) and (11), one gets $\text{VAR}[Z_k^{(2)}]/\mathbb{E}^2[Z_k^{(2)}] \approx 1/(4Q)$ for very large Q . Therefore, as $Q \rightarrow +\infty$, the pdf of $Z_k^{(2)}$ can be approximated by the following Dirac delta distribution $f_{Z_k^{(2)}}(\alpha) \approx \delta(\alpha - \mathbb{E}[Z_k^{(2)}])$, with the mean of $Z_k^{(2)}$ given by (10). Accordingly, relying on the results of the transformations of random variables [8], the pdf of X_k is approximated by

$$f_{X_k}(\alpha) \approx \frac{\sqrt{\alpha - \mathbb{E}[Z_k^{(2)}]}}{\sigma_h^2 \sqrt{\alpha}} e^{-\frac{(\sqrt{\alpha - \mathbb{E}[Z_k^{(2)}]})^2}{\sigma_h^2}}, \quad \text{for } \alpha > \mathbb{E}[Z_k^{(2)}] \quad (18)$$

whereas $f_{X_k}(\alpha) = 0$ for $\alpha \leq \mathbb{E}[Z_k^{(2)}]$. After algebraic manipulations, the cdf of X_k is correspondingly approximated:

$$F_{X_k}(\alpha) \approx 1 - e^{-\frac{(\sqrt{\alpha - \mathbb{E}[Z_k^{(2)}]})^2}{\sigma_h^2}}, \quad \text{for } \alpha > \mathbb{E}[Z_k^{(2)}] \quad (19)$$

whereas $F_{X_k}(\alpha) = 0$ for $\alpha \leq \mathbb{E}[Z_k^{(2)}]$.

For any value of K , the distributions (18) and (19) can be substituted in (9) in order to obtain an approximation of the pdf of α_{opt} , which is involved in the calculus of the average sum-rate capacity (8). On the other hand, since the distribution (19) is a von Mises function,³ one can resort to (16) for sufficiently large values of K , where (13) ends up to

$$b_K = \left[\sigma_f \sigma_g Q + \sigma_h \sqrt{\ln(K)} \right]^2, \quad a_K = \sigma_h^2 + \frac{\sigma_f \sigma_g \sigma_h Q}{\sqrt{\ln(K)}}. \quad (20)$$

B. Approximation 2: Sum of Nakagami variates

The random variable Z_k is the sum of the two independent and non-identically distributed (i.n.i.d.) Nakagami random variables $Z_k^{(1)}$ and $Z_k^{(2)}$. Therefore, the pdf of Z_k is the convolution of the pdfs of $Z_k^{(1)}$ and $Z_k^{(2)}$, which does not admit a closed-form expression. Following [15], we propose to approximate the unknown pdf $f_{Z_k}(\alpha)$ of Z_k by the pdf $f_{\hat{Z}_k}(\alpha)$ of the random variable \hat{Z}_k defined as $\hat{Z}_k \triangleq \sqrt{\left[\hat{Z}_k^{(1)} \right]^2 + \left[\hat{Z}_k^{(2)} \right]^2}$, where $\hat{Z}_k^{(1)}$ and $\hat{Z}_k^{(2)}$ are i.i.d. Nakagami random variables with shape parameter \hat{m} and scale parameter $\hat{\Omega}$, which are determined such that $f_{\hat{Z}_k}(\alpha)$ be an accurate approximation of $f_{Z_k}(\alpha)$. The choice of \hat{m} and $\hat{\Omega}$ will be discussed soon after.

At this point, we would like to point out that the main advantage of using $f_{\hat{Z}_k}(\alpha)$ in lieu of $f_{Z_k}(\alpha)$ stems from the fact that the square of \hat{Z}_k is the sum of two i.i.d. gamma random variables [14]. Indeed, the square of a Nakagami random variable with shape parameter \hat{m} and scale parameter $\hat{\Omega}$ turns out to be a gamma random variable with shape parameter \hat{m} and scale parameter $\hat{\Omega}/\hat{m}$. Moreover, the sum of the two i.i.d. gamma random variables $[\hat{Z}_k^{(1)}]^2$ and $[\hat{Z}_k^{(2)}]^2$ is a gamma random variable, too, with shape parameter $2\hat{m}$ and scale parameter $\hat{\Omega}/\hat{m}$. Thus, we can conclude that the pdf

³The proof is straightforward and, thus, it is omitted.

of the random variable $\widehat{X}_k \triangleq \widehat{Z}_k^2$ is given by (see, e.g., [14])

$$f_{\widehat{X}_k}(\alpha) = \left(\frac{\widehat{m}}{\widehat{\Omega}}\right)^{2\widehat{m}} \frac{\alpha^{2\widehat{m}-1}}{\Gamma(2\widehat{m})} e^{-\frac{\widehat{m}}{\widehat{\Omega}}\alpha}, \quad \text{for } \alpha > 0 \quad (21)$$

whose corresponding cdf reads as $F_{\widehat{X}_k}(\alpha) = P\left(\frac{\widehat{m}\alpha}{\widehat{\Omega}}, 2\widehat{m}\right)$.⁴

1) *Choice of the parameters \widehat{m} and $\widehat{\Omega}$:* To obtain an accurate approximation of $f_{Z_k}(\alpha)$, we resort to the *moment matching* method. Specifically, the parameters \widehat{m} and $\widehat{\Omega}$ are chosen such that to match the second and fourth moments of Z_k and \widehat{Z}_k , i.e., (i) $\mathbb{E}[Z_k^2] = \mathbb{E}[\widehat{Z}_k^2]$ and (ii) $\mathbb{E}[Z_k^4] = \mathbb{E}[\widehat{Z}_k^4]$. By observing that $\mathbb{E}[\widehat{Z}_k^2] = \mathbb{E}[X_k]$, with the mean of the gamma distribution (21) being the ratio between its shape and scale parameters, i.e., $2\widehat{m}/(\widehat{\Omega}/\widehat{m}) = 2\widehat{\Omega}$, condition (i) yields

$$\widehat{\Omega} = \frac{\mathbb{E}[Z_k^2]}{2} = \frac{1}{2} \mathbb{E}[X_k]. \quad (22)$$

Since $\mathbb{E}[\widehat{Z}_k^4] = \mathbb{E}[\widehat{X}_k^2]$, with the 2-nd moment of the gamma random variable \widehat{X}_k given [14] by $\mathbb{E}[\widehat{X}_k^2] = \left(\frac{\widehat{\Omega}}{\widehat{m}}\right)^2 \frac{\Gamma(2\widehat{m}+2)}{\Gamma(2\widehat{m})} = \frac{2\widehat{\Omega}^2}{\widehat{m}}(2\widehat{m}+1)$, where we have also used $\Gamma(x+1) = x\Gamma(x)$, which is in general valid for all complex numbers x except the non-positive integers, condition (ii) leads to

$$\widehat{m} = \frac{1}{2} \frac{\mathbb{E}^2[X_k]}{\mathbb{E}[X_k^2] - \mathbb{E}^2[X_k]} = \frac{1}{2} \frac{\mathbb{E}^2[X_k]}{\text{VAR}[X_k]}. \quad (23)$$

By observing that the moments of the Rayleigh random variable $|h_k|$ and the chi-distributed random variable $\|\mathbf{f}_k\|$ can be expressed as (see, e.g., [8]) $\mathbb{E}[|h_k|^n] = \sigma_h^n \Gamma(1 + \frac{n}{2})$ and $\mathbb{E}[\|\mathbf{f}_k\|^n] = \sigma_f^n \frac{\Gamma(Q + \frac{n}{2})}{\Gamma(Q)}$, for $n \in \mathbb{N}$, the first two moments of X_k are given by

$$\mathbb{E}[X_k] = \sigma_h^2 + \sigma_f^2 \sigma_g^2 Q^2 + \sigma_f \sigma_g \sigma_h \sqrt{Q} \pi \frac{\Gamma(Q + \frac{1}{2})}{\Gamma(Q)} \quad (24)$$

$$\begin{aligned} \mathbb{E}[X_k^2] &= 2\sigma_h^4 + 3\sigma_f \sigma_g \sigma_h^3 \sqrt{Q} \pi \frac{\Gamma(Q + \frac{1}{2})}{\Gamma(Q)} \\ &+ 6\sigma_f^2 \sigma_g^2 \sigma_h^2 Q^2 + 2\sigma_f^3 \sigma_g^3 \sigma_h Q \sqrt{Q} \pi \frac{\Gamma(Q + \frac{3}{2})}{\Gamma(Q)} \\ &+ \sigma_f^4 \sigma_g^4 Q^3 (Q+1) \end{aligned} \quad (25)$$

where we have also observed that $\Gamma(3/2) = \sqrt{\pi}/2$ and $\Gamma(5/2) = 3\sqrt{\pi}/4$. Eqs. (24) and (25) have to be substituted in (22) and (23) in order to completely characterize \widehat{X}_k .

C. Discussion

Let us first consider the case when $K \rightarrow +\infty$ and the reflection channel hardens. In this situation, using (20), the average receive SNR in (17) reads as

$$\bar{\rho}_{\text{sum}} = \bar{\rho}_{\text{sum}}^{\text{w/o RIS}} + \mathcal{P}_{\text{TX}} \left[\sigma_f^2 \sigma_g^2 Q^2 + \sigma_f \sigma_g \sigma_h \frac{2 \ln(K) + C}{\sqrt{\ln(K)}} Q \right]$$

which shows that, compared to the RIS-unaided downlink, the SNR gain provided by the presence of the RIS depends on the relationship between K and Q . Indeed, if Q approaches infinity at the same rate as K , i.e., $Q = \chi K$, where $\chi \neq 0$ is a constant independent of K , it results that $\lim_{K, Q \rightarrow +\infty} \bar{\rho}_{\text{sum}}/Q^2 =$

⁴It can be verified that $F_{\widehat{X}_k}(\alpha)$ is a von Mises function, too.

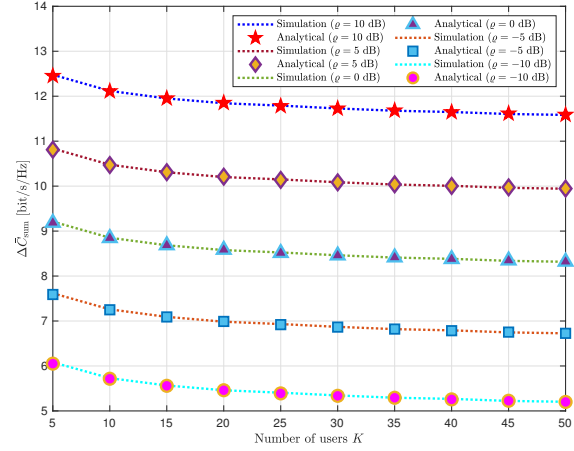


Fig. 1. $\Delta\bar{C}_{\text{sum}}$ versus K (Approximation 2 for the analytical curves).

$\mathcal{P}_{\text{TX}} \sigma_f^2 \sigma_g^2$, i.e., the average receive SNR scales like Q^2 as K and Q grow to infinity. In this case, the downlink performance is dominated by the reflection channel and the reflection process of the RIS becomes predominant with respect to multiuser diversity effects. On the other hand, if Q approaches $+\infty$ as $Q = \chi \sqrt{\ln(K)}$, one has $\lim_{K, Q \rightarrow +\infty} \bar{\rho}_{\text{sum}}/\ln(K) = \mathcal{P}_{\text{TX}} [(\sigma_f \sigma_g \chi + \sigma_h)^2 + C \sigma_f \sigma_g \sigma_h \chi]$. In this case, the sum-rate capacity also depends on the direct channel and the effect of the RIS becomes negligible when $\sigma_f \sigma_g \chi \ll \sigma_h$, thus approaching the performance of the RIS-unaided downlink.

Let us now consider the case when K grows to infinity and hardening of the reflection channel does not hold. In this situation, we resort to the approximation (21) for the distribution of X_k . According to (13), the constant b_K is the solution of $P\left(\frac{\widehat{m}b_K}{\widehat{\Omega}}, 2\widehat{m}\right) = 1 - \frac{1}{K}$, which is given by

$$b_K = \frac{\widehat{\Omega}}{\widehat{m}} P^{-1}\left(1 - \frac{1}{K}, 2\widehat{m}\right) \quad (26)$$

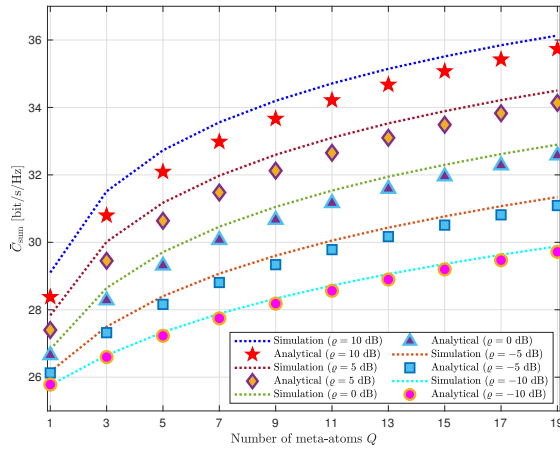
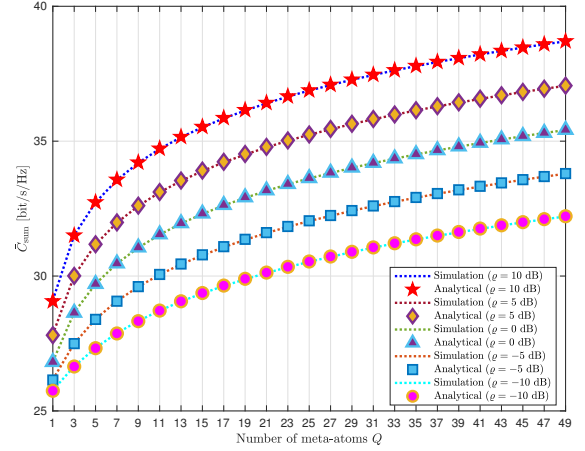
where $P^{-1}(y, a)$ is the inverse of the lower incomplete gamma function for $y \in [0, 1]$, i.e., $P^{-1}(P(x, a), a) = x$. Substituting (26) in (13) and replacing $f_{X_k}(b_K)$ with $f_{\widehat{X}_k}(b_K)$, one has

$$a_K = \frac{\widehat{\Omega}}{\widehat{m}} \frac{\Gamma(2\widehat{m})}{K [P^{-1}(1 - \frac{1}{K}, 2\widehat{m})]^{2\widehat{m}-1} e^{-P^{-1}(1 - \frac{1}{K}, 2\widehat{m})}}. \quad (27)$$

The dependence of (26) and (27) on K and Q will be shown numerically in the forthcoming section.

IV. NUMERICAL PERFORMANCE ANALYSIS

We consider a 2-D Cartesian system, wherein the BS and the RIS are located at $(0, 0)$ and $(10, 0)$ (in meters), respectively, whereas the users form a circular cluster centered in $(40, -10)$ (in meters). The inter-element spacing is fixed to $d_{\text{RIS}} = \lambda_0/4$, whereas the AoA at the RIS is uniformly distributed in $(-\pi/4, \pi/4)$. All the other channel links are independently generated by assuming a carrier frequency $f_0 = 25$ GHz, with variance $\sigma_\alpha^2 = G_\alpha d_\alpha^{-\eta} \lambda_0^2 / (4\pi)^2$, for $\alpha \in \{g, h\}$, where $G_\alpha = 25$ dBi for the RIS and $G_\alpha = 5$ dBi for the UEs, while d_α represents the distance of the link and $\eta = 1.6$ is the path

Fig. 2. \bar{C}_{sum} versus Q ($K = 10$, Approximation 1 for the analytical curves).Fig. 3. \bar{C}_{sum} versus Q ($K = 10$, Approximation 2 for the analytical curves).

loss exponent. The variance σ_f^2 of the channel link between the RIS and the UEs is derived from the ratio $\rho \triangleq (\sigma_f^2 \sigma_g^2) / \sigma_h^2$, which assumes the values in $\{0, \pm 5, \pm 10\}$ dB. The effective isotropic radiated power of the BS is set to 33 dBm and the noise power at the UEs is equal to -100 dBm.

In Fig. 1, we report the difference $\Delta \bar{C}_{\text{sum}} \triangleq \bar{C}_{\text{sum}} - \bar{C}_{\text{sum}}^{\text{w/o RIS}}$ between the average sum-rate capacity of the RIS-aided and RIS-unaided downlinks, as a function of the number of users K for different values of ρ . The rates \bar{C}_{sum} and $\bar{C}_{\text{sum}}^{\text{w/o RIS}}$ are numerically obtained by averaging (4) over 1000 independent Monte Carlo runs and setting in (7) $Q = 30$ for the RIS-aided downlink and $Q = 0$ for the RIS-unaided one, respectively. The corresponding analytical curves (15)-(16) are plotted by using the parameters (26) and (27) (Approximation 2). Besides corroborating the noticeable accuracy of the proposed approximation, which does not require hardening of the reflection channel, it is seen from Fig. 1 that $\Delta \bar{C}_{\text{sum}}$ decreases with K . This behavior is due to the fact that the increase in K of \bar{C}_{sum} is partially hidden by the larger SNR gain due to reflection process of the RIS, while $\bar{C}_{\text{sum}}^{\text{w/o RIS}}$ scales like $\ln(\ln(K))$.

Fig. 2 and 3 depict the performance of the RIS-aided downlink as a function of the number of meta-atoms Q for different values of ρ , with $K = 10$. In this case, $\bar{C}_{\text{sum}}^{\text{w/o RIS}} = 25.26$ dB. In Fig. 2, the rate \bar{C}_{sum} is compared with the analytical curve (15)-(16) by using the parameters (20) (Approximation 1), whereas (26) and (27) (Approximation 2) are used in Fig. 3. Results confirm the precision of Approximation 2 and show that the approximation based on the hardening of the reflection channel (Approximation 1) is inaccurate for small values of Q , especially when the reflection channel is stronger than the direct one. From the comparison among Figs. 1, 2, and 3, it can be inferred that, as predicted, the sum-rate capacity increases much faster with respect to Q than K .

V. CONCLUSIONS

We derived two approximations of the sum-rate capacity of a TDMA downlink with an RIS. The approximation based on the hardening of the reflection channel allows to show the asymptotic scaling laws in terms of the number of users K and the number of meta-atoms Q . A more accurate approximation

was derived by approximating the overall channel seen by each user as a gamma random variable. Both multiuser diversity and reflection process of the RIS provide increased channel magnitudes. However, the SNR gain increases faster with respect to Q than K and, thus, the multiuser diversity effect becomes negligible even for moderate values of Q .

REFERENCES

- [1] T.J. Cui, M.Q. Qi, X. Wan, J. Zhao, and Q. Cheng, "Coding metamaterials, digital metamaterials and programmable metamaterials," *Light-Sci. Appl.*, vol. 3, e218, Oct. 2014.
- [2] M. Di Renzo *et al.*, "Smart radio environments empowered by reconfigurable AI meta-surfaces: An idea whose time has come," *J. Wireless Commun. Network*, 129 (2019).
- [3] M. Di Renzo *et al.*, "Smart radio environments empowered by reconfigurable intelligent surfaces: How it works, state of research, and the road ahead," *IEEE J. Select. Areas Commun.*, vol. 38, pp. 2450-2525, Nov. 2020.
- [4] D.N.C. Tse, "Optimal power allocation over parallel Gaussian channels," in *Proc. Int. Symp. Information Theory*, Ulm, Germany, June 1997.
- [5] M. Sharif and B. Hassibi, "A comparison of time-sharing, DPC, and beamforming for MIMO broadcast channels with many users," *IEEE Trans. Commun.*, vol. 55, pp. 11-15, Jan. 2007.
- [6] F. Verde, D. Darsena, and V. Galdi "Space-time reconfigurable intelligent surfaces for downlink multiuser transmissions", *arXiv:2304.11912*.
- [7] M. Di Renzo, F.H. Danufane, and S. Tretyakov, "Communication models for reconfigurable intelligent surfaces: From surface electromagnetics to wireless networks optimization," *Proc. IEEE*, vol. 110, pp. 1164-1209, Sept. 2022.
- [8] J.G. Proakis, *Digital Communications*. New York, NY, USA: McGraw-Hill, 2001.
- [9] G. Arfken, *Stirling's Series (3rd Ed.)*, in *Mathematical Methods for Physicists*, Orlando, FL: Academic Press, pp. 555-559, 1985.
- [10] M.R. Leadbetter, "Extreme value theory under weak mixing conditions," *Studies in Probability Theory, MAA Studies in Mathematics*, pp. 46-110, 1978.
- [11] E.J. Gumbel, *Statistics of Extremes*. Columbia University Press, 1958.
- [12] S. Kalyani and R.M. Karthik, "The asymptotic distribution of maxima of independent and identically distributed sums of correlated or non-identical gamma random variables and its applications," *IEEE Trans. Commun.*, vol. 60, pp. 2747-2758, Sep. 2012.
- [13] H.Q. Ngo and E.G. Larsson, "No downlink pilots are needed in TDD massive MIMO," *IEEE Trans. Wireless Commun.*, vol. 16, pp. 2921-2935, May 2017.
- [14] G. Casella and R.L. Berger, *Statistical Inference*. Pacific Grove, CA: Duxbury-Thompson Learning, 2002.
- [15] Z. Hadzi-Velkov, N. Zlatanov, and G.K. Karagiannidis, "An accurate approximation to the distribution of the sum of equally correlated Nakagami- m envelopes and its application in equal gain diversity receivers," in *Proc. IEEE Int. Conf. Commun. (ICC)*, Dresden, Germany, June 2009, pp. 1-5.